



### Science Arts & Métiers (SAM)

is an open access repository that collects the work of Arts et Métiers Institute of Technology researchers and makes it freely available over the web where possible.

This is an author-deposited version published in: <https://sam.ensam.eu>  
Handle ID: [.http://hdl.handle.net/10985/24841](http://hdl.handle.net/10985/24841)

#### To cite this version :

Faissal CHEGDANI, Mohamed EL MANSORI - Effect of the measurement contact scale on the thermomechanical characterization of biocomposite surfaces - Surface Topography: Metrology and Properties - Vol. 11, n°1, p.014009 - 2023

Any correspondence concerning this service should be sent to the repository

Administrator : [scienceouverte@ensam.eu](mailto:scienceouverte@ensam.eu)



# Effect of the measurement contact scale on the thermomechanical characterization of biocomposite surfaces

Faissal CHEGDANI<sup>a,\*</sup>, Mohamed EL MANSORI<sup>a,b</sup>

<sup>a</sup> Arts et Métiers Institute of Technology, MSMP, HESAM Université, F-51006 Châlons-en-Champagne, France

<sup>b</sup> Texas A&M Engineering Experiment Station, Institute for Manufacturing Systems, College Station, TX 77843, USA.

## **Abstract**

This paper proposes a multiscale surface characterization of biocomposites using the nanoindentation technique to identify the functional relationship between the measurement contact scale and the thermomechanical response of each biocomposite component, typically natural plant fibers and the polymer matrix. Flax fiber reinforced polypropylene composites are considered in this investigation. The measurement contact scale in nanoindentation is monitored by the tip indenter radius that ranges from ~ 10 nm to ~ 400 nm using different nanoindentation devices (AFM and commercial triboindenters). The thermal contribution is considered by heating the samples during the nanoindentation experiments. Finally, the outputs from multiscale nanoindentation experiments are confronted with the thermomechanical properties reported in the literature with conventional tensile tests as a reference. The results of this paper show the fundamental importance of considering contact scale measurement when characterizing the mechanical properties of biocomposites. Indeed, flax fibers are highly affected by the geometrical contact scale of indentation, while polypropylene does not show a significant dependence on the contact scale. On the other side, flax fibers show a specific multiscale thermomechanical behavior that is related to their hygrometric properties.

## **Keywords**

Biocomposites; Plant fibers; Nanoindentation; Atomic Force Microscopy; Tribo-indenter; Elastic modulus.

---

\* Corresponding author: F. Chegdani  
E-mail: [faissal.chegdani@ensam.eu](mailto:faissal.chegdani@ensam.eu)  
ORCID: [0000-0002-7643-9701](https://orcid.org/0000-0002-7643-9701)

## 1. Introduction

Biocomposite materials made with natural plant fibers are recognized by both scientific and industrial communities as a viable alternative to synthetic fiber composites thanks to many economic, ecological, and technical advantages [1–5]. Indeed, some types of plant fibers have mechanical properties similar to synthetic glass fibers while being lighter [3,6]. Plant fibers present also other technical properties such as thermal insulation and soundproofing [7]. On the other hand, polypropylene (PP) is widely used as a matrix material for natural fiber composites because it possesses several useful properties like high heat distortion temperature, transparency, flame resistance, dimensional stability, and high impact strength [8].

However, the use of biocomposites in the industry shows some limitations because of the high variability of their mechanical properties, which complicates compliance with industrial specifications [9]. The high variability of the mechanical properties of biocomposites can be attributed in part to the multiscale structure of the plant fibrous reinforcement that induces different mechanical responses at each scale level. Indeed, the plant fibrous reinforcements have different structures at each scale: cellulose microfibrils at the nanoscale, elementary fibers at the microscale, fiber bundles at the mesoscale, and an assembly of fiber bundles and polymer matrix at the macroscale. As shown in Figure 1(a), plant fibers are mechanically extracted from plant stem in form of bundles by breaking and scutching [10]. In order to improve both the mechanical properties of the fibrous structure and the cohesion between the fibrous structure and the polymer matrix, fiber bundles are separated into smaller bundles by hackling [10]. These small bundles are called technical fibers and are the basic form used to perform fibrous reinforcement in the composite industry. Technical fibers are composed of elementary fibers naturally gathered by the so-called middle lamella [11].

Elementary fibers consist of a stack of a primary cell wall (P in Figure 1(b)) and a secondary cell wall (S in Figure 1(b)) arranged as concentric cylinders with a small channel in the middle called a lumen [12]. The secondary cell wall is divided into three layers (S1, S2, and S3 in Figure 1(b)). The bulk of the fiber is essentially constituted by layer S2 of the secondary cell wall [12]. Each cell wall is itself a composite structure that contains cellulose microfibrils embedded in amorphous polymers, typically hemicellulose and lignin [13]. These elementary fiber components show a significant difference in terms of mechanical properties. For example, the elastic modulus of crystalline cellulose is in the range of 120 – 138 GPa, while it has been reported that the elastic modulus is in the range of 3.5 – 8 GPa for hemicellulose and in the range of 2 – 6.7 GPa for lignin [12,14]. For elementary flax fibers, the elastic modulus is in the range of 28 – 100 GPa [9]. As reported in [15], the mechanical behavior of bundles differs from that of elementary fibers as the former are bonded assemblies of elementary fibers with a hierarchy of interfaces.

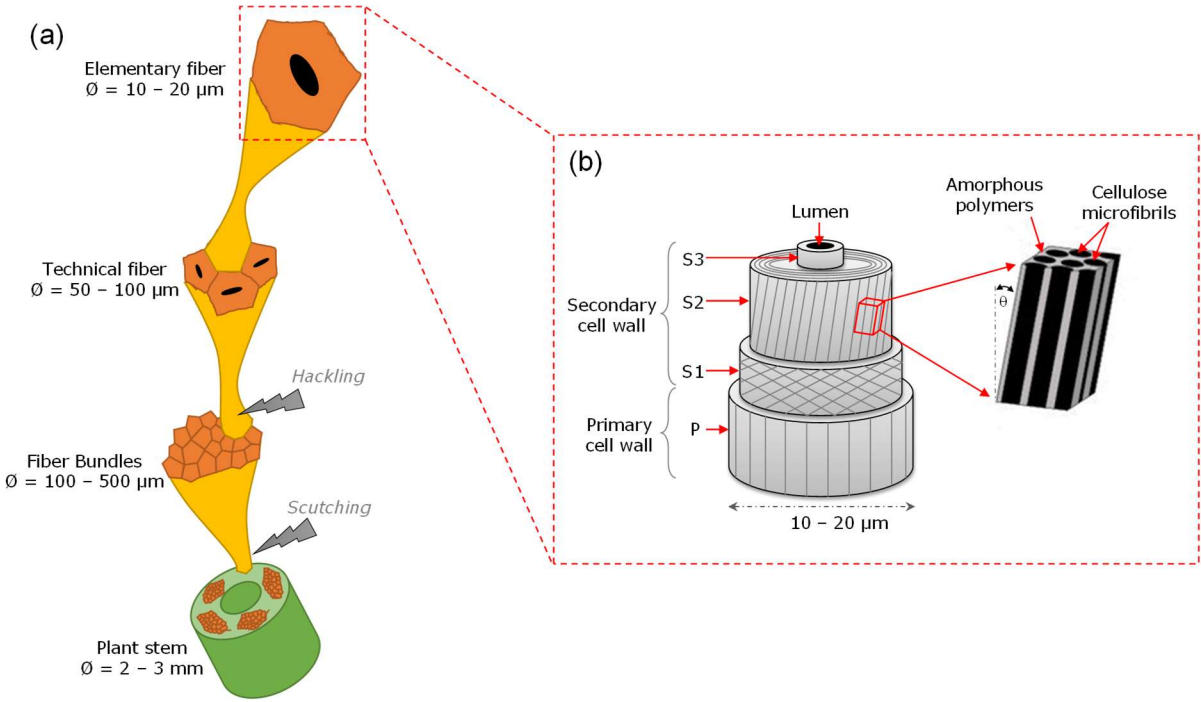


Figure 1 : (a) multiscale plant fibrous structure from plant stem to elementary fiber [16], (b) Schematic depiction of elementary plant fiber [17]

It can be concluded from this literature synthesis that the influence of the multiscale organization of the plant fibrous reinforcements on their stiffness variability is associated with the fact that the stiffness of elementary fibers (at the microscale) will depend on the rate of cellulose microfibrils (at the nanoscale) which is present in variable proportions on the fibers due to many natural and environmental factors [12], and the stiffness of the fiber bundles (mesoscale) will depend on the numbers of elementary fibers in the bundle which is also variable.

The thermomechanical response of flax fibers depends hence on the mechanical analysis scale and the contribution of each fiber component to the thermomechanical response at this analysis scale. In this context, this paper aims to conduct a multiscale thermomechanical characterization of a biocomposite made of unidirectional flax fibers and polypropylene matrix using the nanoindentation technique. Nanoindentation has been considered in this study rather than conventional tensile tests because it allows targeting locally and separately each phase of the biocomposite material at different scale levels to obtain fundamental mechanical property parameters. The multiscale aspect is investigated in this study by monitoring the geometrical contact scale of nanoindentation, typically the tip indenter radius. Since tensile tests are the most conventional method to characterize mechanical properties, the multiscale results of nanoindentation are then confronted with those of tensile tests from literature data as a reference.

## **2. Experimental approach**

The biocomposite considered in this work is supplied by Composites Evolution — UK. The commercial name of the biocomposite is Biotex Flax/PP UD. It is composed of unidirectional long flax fibers and polypropylene (PP) matrix as continuous warp flax yarns. The volume fraction of flax fibers in the biocomposite is around 40%. As shown

in the illustration of Figure 2(a), flax fibers are perpendicular to the worksurface in order to work on the cross-section of fibers.

All the worksurfaces have been prepared through three steps of water-lubricated polishing with a progressive decrease of the sandpaper grit size: 1 min with a grit size of 18  $\mu\text{m}$ , 2 min with a grit size of 10  $\mu\text{m}$ , and 3 min with a grit size of 5  $\mu\text{m}$ . Polished samples are then left to dry for 48 hours at room temperature. It is important to note that biocomposites are affected by humidity due to their hydrophilic nature which is well-known in the literature [18–20]. However, this phenomenon has not been considered in this work since the exposition time to water during the polishing process is too short (6 minutes) to induce a significant water absorption in the composite. It has been shown in the literature that biocomposites need at least  $\sim 10$  hours of water immersion to start seeing a weight change in the biocomposite samples and about 1 week of water immersion to see a variation of the elastic modulus due to moisture content [20].

To characterize the mechanical properties of each biocomposite component at different contact scale levels, nanoindentation has been chosen in this study because it allows targeting each biocomposite phase independently of others. Thus, elementary flax fibers can be indented separately from the polymer matrix and vice-versa as can be shown in Figure 2(b) and Figure 2(c) with the pyramidal indentation traces made by the tip indenter. This pyramidal trace is the shape of the well-known Berkovich tip indenters illustrated in Figure 3(a). At the vertex of this tip indenter, the tip radius ( $R$ ) shown in Figure 3(b) represents the geometrical contact scale with which the mechanical indentation contact is engaged.

As shown in Figure 3(c), the nanoindentation technique involves the normal contact of an indenter on a worksurface and its penetration in this surface to a specified load or

depth [21]. The load is measured regarding the displacement into the worksurface to get the load–penetration curve shown in Figure 3(d). The relevant parameters for the nanoindentation analysis are the maximum displacement ( $h_{max}$ ), the maximum load on the sample ( $F_{max}$ ), and the contact stiffness ( $S$ ) which is the slope of the tangent line to the unloading curve at the maximum loading point as illustrated in Figure 3(d).

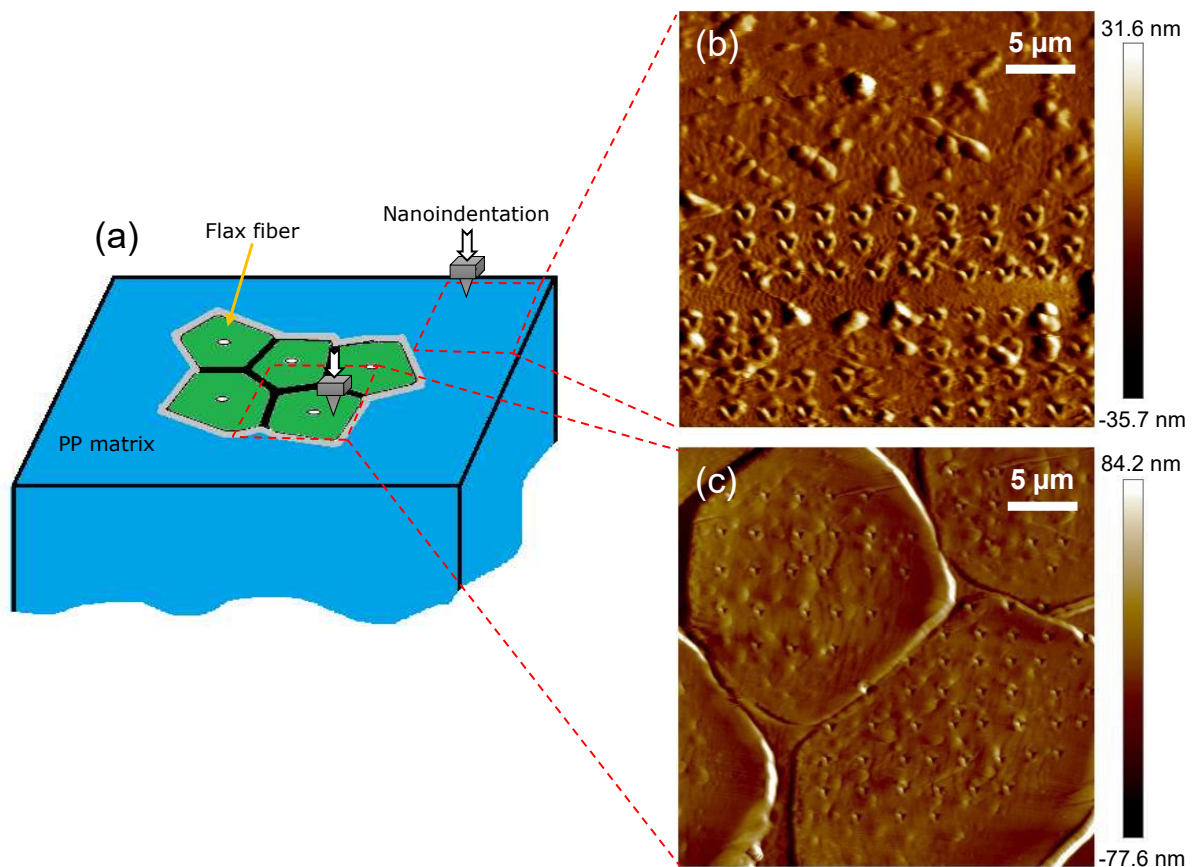


Figure 2: (a) Schematic representation of a biocomposite structure showing a technical flax fiber embedded in a PP matrix. (b) AFM scanning image of PP matrix showing the indentation traces. (c) AFM scanning image of flax fibers showing the indentation traces

Nanoindentation analysis is usually performed with the model of Oliver & Pharr [22] in the case of Berkovich indenters to estimate the elastic modulus of the work-material from the indentation curve [23–26]. It consists of computing the contact depth ( $h_c$ ) which is dependent on the material deformation and the tip shape as shown in Figure 3(c).  $h_c$  can be calculated using Eq (1) where  $\varepsilon$  is a constant related to the tip geometry

(0.72 for Berkovich tip [21]). The projected contact area of nanoindentation ( $A$ ) can be calculated using Eq (2). Then, the reduced elastic modulus is obtained using Eq (3) where  $\beta$  is a constant related to the tip geometry (1.034 for Berkovich tip [21]). The elastic modulus of the work-material can be calculated with Eq (4) where  $E_i$  and  $\nu_i$  are respectively the elastic modulus and the Poisson coefficient of the tip indenter.  $\nu$  is the Poisson coefficient of the indented material.

$$h_c = h_{max} - \varepsilon \frac{F_{max}}{S} \quad (1)$$

$$A = 24.56 \times h_c^2 \quad (2)$$

$$E_r = \frac{S\sqrt{\pi}}{2\beta\sqrt{A}} \quad (3)$$

$$\frac{1}{E_r} = \frac{(1 - \nu^2)}{E} + \frac{(1 - \nu_i^2)}{E_i} \quad (4)$$

The geometrical contact scale has been monitored in this study by the tip indenter radius ( $R$ ). To investigate a large range of tip indenter radii, different indenter devices have been used as shown in Figure 4. Nanoindentation with an Atomic force microscope (AFM) allows using indenters with tip radii that can reach  $\sim 10$  nm. The commercial Bruker Hysitron triboindenter is suitable for tip radii in the range of 100 – 150 nm, while the commercial MTS Nanoindenter XP can work with tip indenters that have tip radii of  $\sim 400$  nm. Therefore, 5 values of tip indenter radii are considered in this study as follows: 10 nm, 40 nm, 100 nm, 150 nm, and 400 nm.



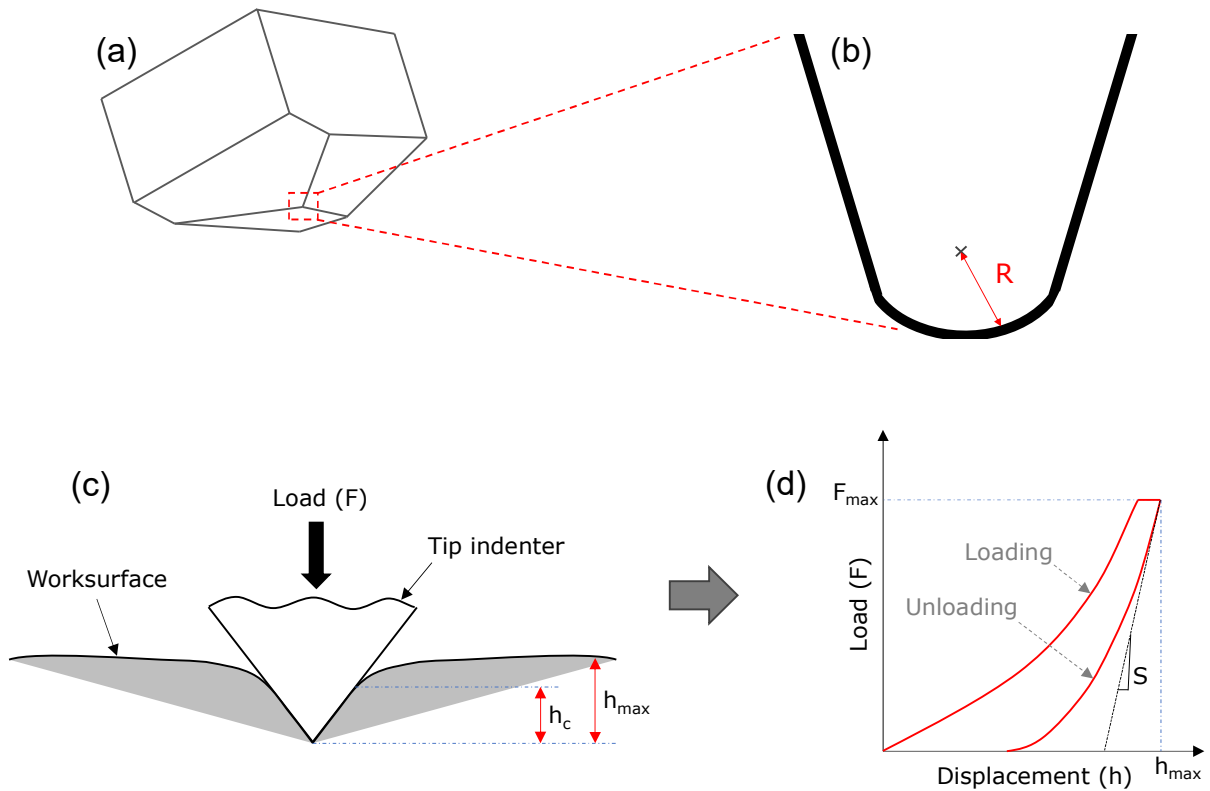


Figure 3: (a) Berkovich tip indenter shape. (b) Schematic illustration of the tip indenter radius. (c) Schematic depiction of the indentation process showing the characteristic depths. (d) Loading/unloading curves obtained from nanoindentation

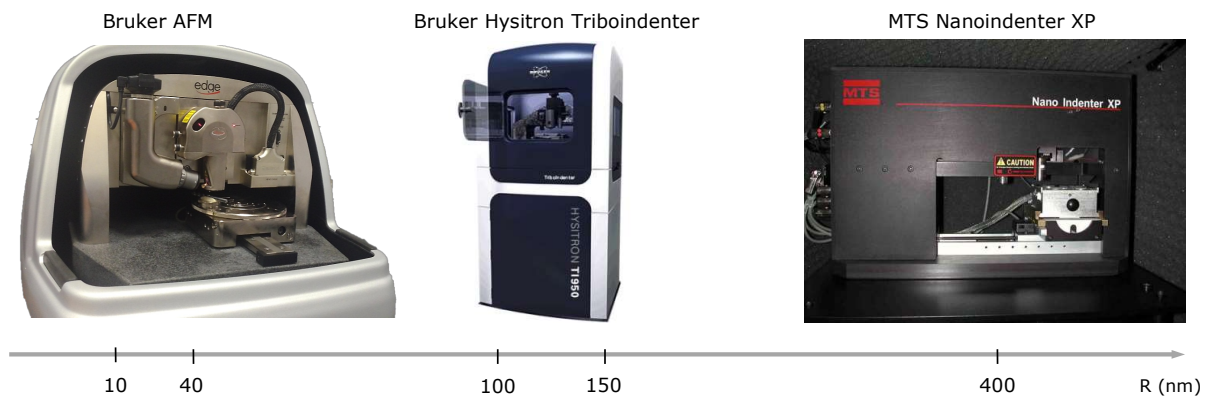


Figure 4: Instruments used for nanoindentation experiments in the function of the considered tip indenter radii

Figure 5 shows the experimental setup for the thermomechanical analysis. A biocomposite sample of 1 mm of thickness is clamped between two heating elements that control the temperature of the active zone. The temperature reached in this active zone is measured with thermocouples and the nanoindentation experiments are performed once the desired temperature is reached. For the thermomechanical analysis, only the indenter with a tip radius of 150 nm was used on the Bruker Hysitron

Triboindenter because they are the only indenter and device adapted for the thermal setup. All the tests have been made at the same room condition and the same conditioning time (15 min). The average room humidity was 60% and the average room temperature was 25°C.

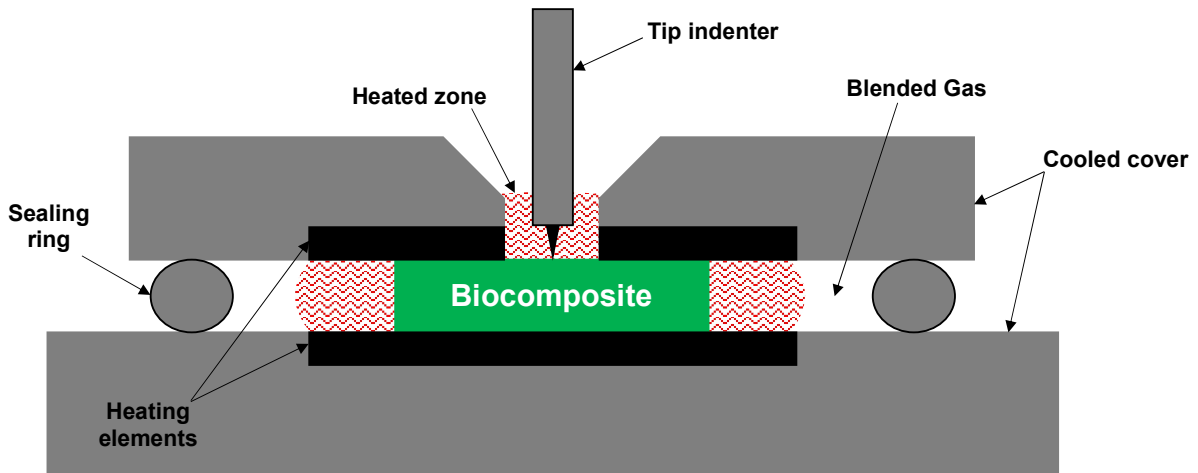


Figure 5: Schematic depiction of the thermal setup used for nanoindentation experiments

Before each nanoindentation experiment, the worksurface is scanned using the scanning probe of the corresponding device so the biocomposite components (fibers and matrix) can be targeted separately as shown in Figure 2(b) and Figure 2(c). On flax fibers, between 10 and 35 indentations are performed on the same fiber depending on the fiber section dimensions. On the PP matrix, between 55 and 60 indentations are performed on the same scanned surface. Each nanoindentation configuration is repeated 5 to 6 times at different locations on the worksurface in order to ensure repeatability. Thus, the output values from nanoindentation experiments are presented as the mean of these repeated tests. Errors are considered as the average of the absolute deviations of data repeatability tests from their mean.

### 3. Results and discussion

#### 3.1. Effect of the measurement contact scale on the indentation behavior

Figure 6 shows the indentation curves obtained for flax fibers and PP matrix with tip radii of 100 nm and 150 nm. The applied loading instruction has been fixed to 500  $\mu\text{N}$ . This value has been achieved with a tip radius of 150 nm while the indentation with a tip radius of 100 nm does not exceed 450  $\mu\text{N}$ . It can be seen from Figure 6 that changing the Berkovich tip indenter radius from 100 nm to 150 nm reduces the indentation depth by 46% for flax fibers (Figure 6(a)) and by 17% for the PP matrix (Figure 6(b)). Flax fibers show hence a strong dependence on the indentation contact size compared to the PP matrix where the increase of the tip indenter radius leads to an important increase in the flax fiber resistance to the indentation loading. This specific behavior will be investigated in depth in the next section.

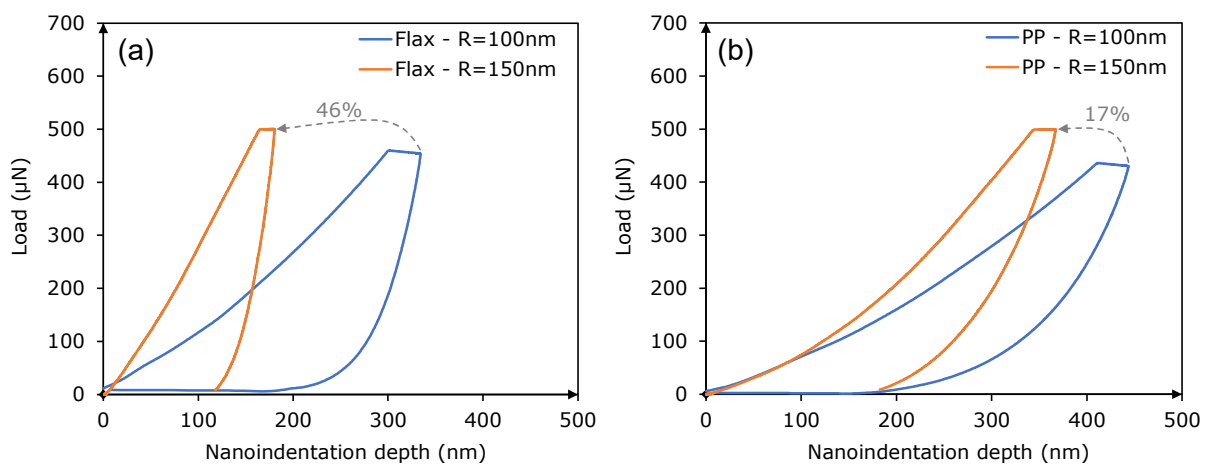


Figure 6: Load-unload curves obtained with nanoindentation experiments showing the effect of the tip indenter radius on (a) flax fibers and (b) PP matrix

### 3.2. Effect of measurement contact scale on the elastic properties

To analyze the effect of the indentation contact scale on the mechanical response of flax fibers and PP matrix, Figure 7 presents the elastic modulus calculated from the indentation curves with the Oliver & Pharr model described in section 2. Results from indentation experiments with different tip edge radii are confronted in Figure 7 with the results of conventional tensile tests obtained from the literature for elementary flax fibers [27] and PP matrix [28].

Figure 7 shows a significant scale effect for the mechanical characterization of flax fibers. The increase of the tip edge radius from 10 nm to 400 nm leads to an increase of the average elastic modulus from 0.42 GPa to 15.5 GPa for flax fibers, and from 1 GPa to 2.5 GPa for the PP matrix. The increase of the tip edge radius leads to a considerable increase in the elastic modulus of flax fibers to approach the values obtained with conventional tensile tests that are around  $52.5^{\pm 8.6}$  GPa based on the results of [27] but can vary from 28 to 100 GPa as reported in [9]. In contrast, the tensile modulus of the PP matrix ( $1.8^{\pm 0.2}$  GPa [28]) is in the range of values obtained with nanoindentation (1 – 2.5 GPa). Literature works on nanoindentation of PP matrix have reported an average elastic modulus of 1.85 GPa with the same nanoindentation technique of this study (single-step nanoindentation) [29], and 3 GPa with the continuous nanoindentation method [30]. The literature variability of PP modulus could be due to the difference in the nanoindentation method, or to the difference in the molecular weight and crystallinity of each PP type [30].

It is important to mention that the polishing technique contributes to the enlargement of the voids and the deformation of the matrix with a consequent increase of the porosity, which has been attributed to the higher applied shear forces compared to other preparation techniques such as microtome [31]. Therefore, the elastic modulus of biocomposite components obtained by nanoindentation could be affected by the polishing process but the trend in the function of the tip indenter radius should be the same since all the surfaces are polished similarly.

The specific mechanical behavior of flax fibers in the function of the measurement contact scale of nanoindentation could be due to their multiscale complex structure shown in Figure 1. Indeed, when indenting with a small tip indenter radius, the most probable hypothesis is that cellulose microfibrils (that have the highest mechanical

properties) are not solicited because of their transverse deformation as shown in Figure 7(a). With the increase of the tip indenter radius, cellulose microfibrils are involved in the indentation contact by compression as shown in Figure 7(b). Increasing the tip indenter radius rises the involvement rate of cellulose microfibrils, which contributes to an increase in the elastic modulus obtained by nanoindentation. In the case of conventional tensile tests, all the cellulose microfibrils are involved by tension in the mechanical load as shown in Figure 7(c). This could explain the highest values of elastic modulus found with tensile tests for flax fibers.

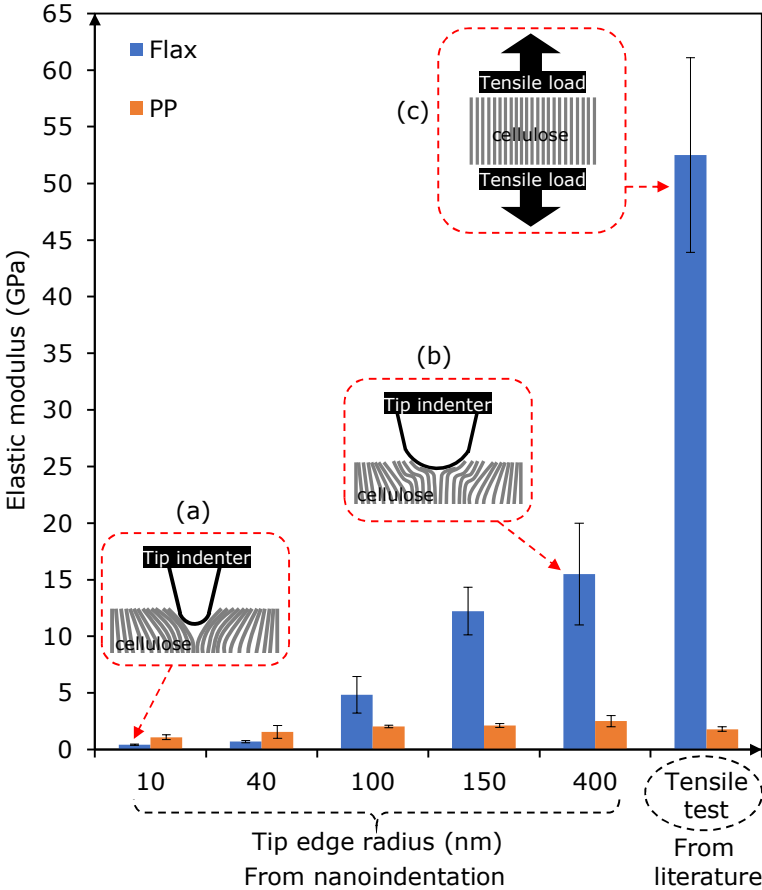


Figure 7: Elastic modulus of flax fibers and PP matrix obtained from nanoindentation experiments with different tip edge radii. Results of tensile tests obtained from the literature [27,28] are given as a reference.

### 3.3. Effect of measurement contact scale on the thermomechanical behavior

Figure 8(a) shows the elastic modulus of flax fibers obtained from nanoindentation experiments with a tip indenter radius of 150 nm at different applied loads and different

sample temperatures. The effect of the applied load is not highly significant when considering the standard deviation of measurements. However, flax fibers show a specific thermomechanical behavior where the elastic modulus increases when increasing the temperature from 25°C to 60°C. Then, the elastic modulus of flax fibers decreases from 60°C to 100°C. This thermomechanical behavior at the nano-contact scale could be attributed to the hygro-mechanical properties of flax fibers. Indeed, flax fibers have a water content in their composition which is in the range of 8 – 12 % [6]. This moisture content contributes to a reduction in the elastic modulus of fibers by a plasticization of their amorphous components [32–34]. Therefore, the increase in temperature from 25°C to 60°C leads to a water release from fibers, which participates in an increase of the elastic modulus by the stiffening of their amorphous components. From 60°C, the decrease of the elastic modulus in the function of temperature increase could be due to the progressive thermal softening of the amorphous components of flax fiber, especially hemicellulose, and lignin. It has been shown in [35] that softening temperatures of the lignin and the hemicellulose were decreased by the presence of water molecules to reach values of about 55°C for hemicellulose and about 72°C for lignin.

On the other hand, the elastic tensile modulus of flax fibers reported from literature in Figure 8(b) shows also a particulate thermomechanical behavior at the microscale. The elastic tensile modulus decreases in the function of temperature from 20°C to 60°C and becomes then stable above 60°C. This specific behavior has also been attributed by the authors to the influence of the water in the fiber than to the temperature effect because they found that the evolution of the mass loss of flax fibers with temperature does not reveal any destruction of the essential components of the fiber in the considered range of temperature [36]. However, in contrast to the nanoindentation

process, the mechanical behavior of flax fibers with tensile tests is rather controlled by cellulose microfibrils than by amorphous fiber components since the cellulose microfibrils are oriented in the longitudinal direction of elementary fibers. The water content in plant fibers leads to an increase in the elastic modulus by hygrometric hardening due to the rearrangements of cellulose microfibrils toward the fiber axis [37]. Indeed, water molecules could induce plasticizing of the amorphous component and the creep of cellulose microfibrils in the relaxed amorphous fiber region, leading to their rearrangements toward the fiber axis [37]. This contributes to a decrease in the microfibrillar angle as reported in [38]. Consequently, the progression of water release from fibers between 20°C and 60°C could be the origin of the reduction of tensile modulus shown in Figure 8(b). The hygrometric effect disappears after water release (above 60°C), which explains the stabilization of the elastic tensile modulus above this critical temperature.

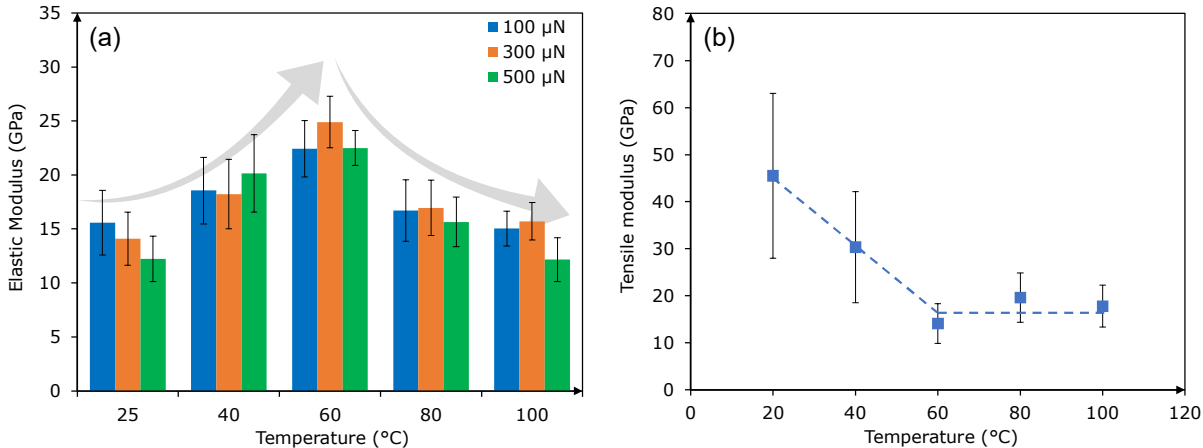


Figure 8: (a) Elastic modulus calculated from nanoindentation of flax fibers in the function of the sample temperature for different values of the applied load. (b) Elastic modulus reported from literature with conventional tensile tests of flax fibers in the function of sample temperature [36].

In the case of the PP matrix, Figure 9(a) shows that the elastic modulus obtained from nanoindentation decreases significantly in the function of sample temperature. The increase of the applied load contributes also to decreasing the elastic modulus. The tensile elastic modulus of PP reported in the literature (Figure 9(b)) shows the same

behavior as that calculated from nanoindentation measurements (Figure 9(a)). Magnitudes of tensile elastic moduli of the PP matrix are close to those acquired with a high applied load in the case of nanoindentation (500  $\mu\text{N}$  in Figure 9(a)). Hence, the thermomechanical behavior of the PP matrix does not show a significant measurement scale effect. This thermomechanical behavior is well-known in the case of thermoplastic polymers because of the thermal softening phenomenon that induces a strong decrease in the polymer stiffness [39,40], especially for PP that is characterized by a glass transition temperature lower than that of the ambient temperature (between  $-23^{\circ}\text{C}$  and  $-10^{\circ}\text{C}$ ) [41].

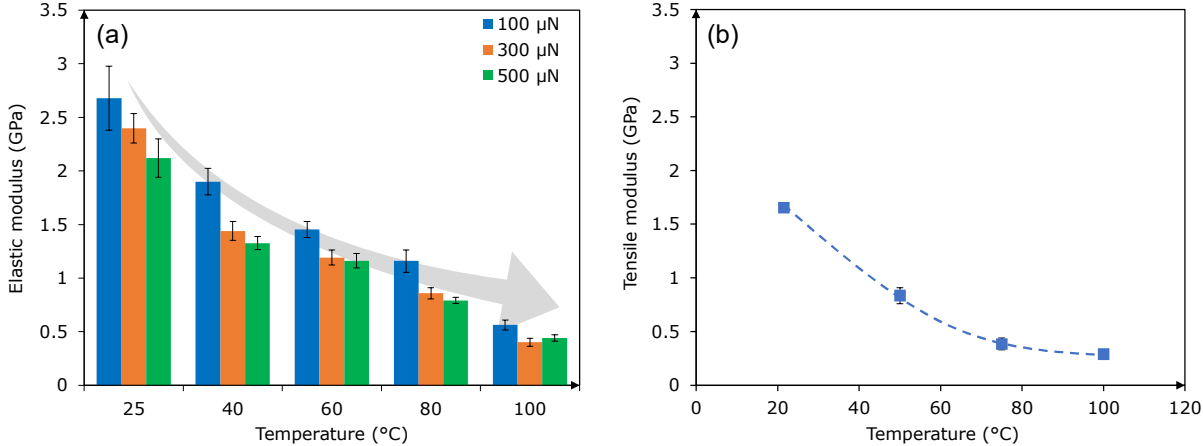


Figure 9: (a) Elastic modulus calculated from nanoindentation of PP matrix in the function of the sample temperature for different values of the applied load. (b) Elastic modulus reported from literature with conventional tensile tests of PP matrix in the function of sample temperature [42].



#### 4. Conclusions

This paper aims to characterize the multiscale thermo-mechanical behavior of biocomposites made with unidirectional flax fibers and polypropylene matrix using the nanoindentation technique. The multiscale analysis concerns the monitoring of the measurement contact scale of the nanoindentation process by varying the edge radius of the tip indenter. The resulting outputs have been confronted with the thermomechanical properties reported in the literature with conventional tensile tests as a reference. The following conclusions can be drawn:

- Flax fibers show a high heterogeneity because of their complex morphology that is considered as a cellulosic composite structure at the micro- and nanoscale.
- The mechanical response of flax fibers is intimately dependent on the geometrical contact scale of the mechanical characterization. Increasing the geometrical contact scale from 10 nm to 400 nm increases the average elastic modulus of flax fibers respectively from 0.42 GPa to 15.5 GPa, which was attributed to the increase of cellulose microfibrils content that is involved in the mechanical contact.
- The thermomechanical properties of flax fibers are differently affected by their moisture content in the function of the measurement contact scale, which is related to the hydrophilic properties. The elastic modulus of flax fibers shows an increase from 25°C to 60°C, and then a decrease from 60°C to 100°C. A characteristic temperature of 60°C has been identified as the water release temperature that induces a modification of the mechanical behavior of flax fibers.
- Mechanical and thermomechanical behaviors of polypropylene matrix from nanoindentation experiments do not show a significant measurement scale effect and correspond to the literature data obtained from conventional tensile tests.

## 5. References

- [1] Akampumuza O, Wambua P M, Ahmed A, Li W and Qin X-H H 2017 Review of the applications of biocomposites in the automotive industry *Polym. Compos.* **38** 2553–69
- [2] Omrani E, L. Menezes P and K. Rohatgi P 2016 State of the art on tribological behavior of polymer matrix composites reinforced with natural fibers in the green materials world *Eng. Sci. Technol. an Int. J.* **19** 717–36
- [3] Pickering K L, Aruan Efendy M G and Le T M 2016 A review of recent developments in natural fibre composites and their mechanical performance *Compos. Part A Appl. Sci. Manuf.* **83** 98–112
- [4] Shalwan A and Yousif B F 2013 In State of Art: Mechanical and tribological behaviour of polymeric composites based on natural fibres *Mater. Des.* **48** 14–24
- [5] Sundeep D, Varadaraj E K, Ephraim S D, Sastry C C and Krishna A G 2022 Mechanical, morphological and thermal analysis of unidirectional fabricated sisal/flax hybrid natural fiber composites *Surf. Topogr. Metrol. Prop.* **10** 015028
- [6] Dittenber D B and GangaRao H V S 2012 Critical review of recent publications on use of natural composites in infrastructure *Compos. Part A Appl. Sci. Manuf.* **43** 1419–29
- [7] Alves C, Ferrao P M C, Silva A J, Reis L G, Freitas M, Rodrigues L B and Alves D E 2010 Ecodesign of automotive components making use of natural jute fiber composites *J. Clean. Prod.* **18** 313–27
- [8] Shubhra Q T H, Alam A K M M and Quaiyyum M A 2013 Mechanical properties of polypropylene composites: A review *J. Thermoplast. Compos. Mater.* **26** 362–91
- [9] Shah D U 2013 Developing plant fibre composites for structural applications by optimising composite parameters: a critical review *J. Mater. Sci.* **48** 6083–107
- [10] Bos H L, Molenveld K, Teunissen W, van Wingerde A M and van Delft D R V 2004 Compressive behaviour of unidirectional flax fibre reinforced composites *J. Mater. Sci.* **39** 2159–68
- [11] Moudood A, Rahman A, Öchsner A, Islam M and Francucci G 2019 Flax fiber and its composites: An overview of water and moisture absorption impact on their performance *J. Reinf. Plast. Compos.* **38** 323–39
- [12] Baley C 2002 Analysis of the flax fibres tensile behaviour and analysis of the tensile stiffness increase *Compos. - Part A Appl. Sci. Manuf.* **33** 939–48
- [13] Lefeuvre A, Bourmaud A, Lebrun L, Morvan C and Baley C 2013 A study of the yearly reproducibility of flax fiber tensile properties *Ind. Crops Prod.* **50** 400–7
- [14] Youssefian S and Rahbar N 2015 Molecular origin of strength and stiffness in bamboo fibrils *Sci. Rep.* **5** 1–13
- [15] Baley C, Gomina M, Breard J, Bourmaud A and Davies P 2020 Variability of mechanical properties of flax fibres for composite reinforcement. A review *Ind. Crops Prod.* **145** 111984
- [16] Chegdani F and Mansori M El 2021 Machining Behavior of Natural Fiber

- Composites *Encycl. Mater. Compos.* **3** 168–85
- [17] Chegdani F, El Mansori M, T. S. Bukkapatnam S and Reddy J N 2019 Micromechanical modeling of the machining behavior of natural fiber-reinforced polymer composites *Int. J. Adv. Manuf. Technol.* **105** 1549–61
- [18] El Hachem Z, Céline A, Challita G, Moya M J and Fréour S 2019 Hygroscopic multi-scale behavior of polypropylene matrix reinforced with flax fibers *Ind. Crops Prod.* **140** 111634
- [19] de Kergariou C, Saidani-Scott H, Perriman A, Scarpa F and Le Duigou A 2022 The influence of the humidity on the mechanical properties of 3D printed continuous flax fibre reinforced poly(lactic acid) composites *Compos. Part A Appl. Sci. Manuf.* **155** 106805
- [20] Le Duigou A, Bourmaud A and Baley C 2015 In-situ evaluation of flax fibre degradation during water ageing *Ind. Crops Prod.* **70** 190–200
- [21] Bourmaud A and Pimbert S 2008 Investigations on mechanical properties of poly(propylene) and poly(lactic acid) reinforced by miscanthus fibers *Compos. Part A Appl. Sci. Manuf.* **39** 1444–54
- [22] Oliver W C and Pharr G M 1992 An Improved Technique for Determining Hardness and Elastic-Modulus Using Load and Displacement Sensing Indentation Experiments *J. Mater. Res.* **7** 1564–83
- [23] Ren L, Cheng Y, Han Z, Meng X and Yang J 2019 Investigation on the mechanical performance of the electroless Ni-W-P coating based on fractal theory *Surf. Topogr. Metrol. Prop.* **7** 025017
- [24] Ebrahimzadeh I, Ashrafizadeh F and Sadeghi B 2019 Scratch and indentation adhesion characteristics of multilayered PVD coatings before and after the heat treatment deposited by duplex process *Surf. Topogr. Metrol. Prop.* **7** 045014
- [25] Arnould O, Siniscalco D, Bourmaud A, Le Duigou A and Baley C 2017 Better insight into the nano-mechanical properties of flax fibre cell walls *Ind. Crops Prod.* **97** 224–8
- [26] Siniscalco D, Arnould O, Bourmaud A, Le Duigou A and Baley C 2018 Monitoring temperature effects on flax cell-wall mechanical properties within a composite material using AFM *Polym. Test.* **69** 91–9
- [27] Baley C and Bourmaud A 2014 Average tensile properties of French elementary flax fibers *Mater. Lett.* **122** 159–61
- [28] Eirasa D and Pessan L A 2009 Mechanical properties of polypropylene/calcium carbonate nanocomposites *Mater. Res.* **12** 517–22
- [29] Gao S L and Mäder E 2002 Characterisation of interphase nanoscale property variations in glass fibre reinforced polypropylene and epoxy resin composites *Compos. - Part A Appl. Sci. Manuf.* **33** 559–76
- [30] Lee S H, Wang S, Pharr G M and Xu H 2007 Evaluation of interphase properties in a cellulose fiber-reinforced polypropylene composite by nanoindentation and finite element analysis *Compos. Part A Appl. Sci. Manuf.* **38** 1517–24
- [31] de Kergariou C, Le Duigou A, Popineau V, Gager V, Kervoelen A, Perriman A, Saidani-Scott H, Allegri G, Panzera T H and Scarpa F 2021 Measure of porosity in flax fibres reinforced polylactic acid biocomposites *Compos. Part A Appl. Sci. Manuf.* **141** 106183
- [32] Chilali A, Zouari W, Assarar M, Kebir H and Ayad R 2018 Effect of water

- ageing on the load-unload cyclic behaviour of flax fibre-reinforced thermoplastic and thermosetting composites *Compos. Struct.* **183** 309–19
- [33] Le Duigou A, Davies P and Baley C 2009 Seawater ageing of flax/poly(lactic acid) biocomposites *Polym. Degrad. Stab.* **94** 1151–62
- [34] Dhakal H N N, Zhang Z Y Y and Richardson M O W O W 2007 Effect of water absorption on the mechanical properties of hemp fibre reinforced unsaturated polyester composites *Compos. Sci. Technol.* **67** 1674–83
- [35] Goring D A I 1965 Thermal softening, adhesive properties and glass transitions in lignin, hemicellulose and cellulose *Consol. Pap. Web, Trans. IIIrd Fund. Res. Symp. Cambridge* 555–68
- [36] Thuault A, Eve S, Blond D, Bréard J and Gomina M 2014 Effects of the hygrothermal environment on the mechanical properties of flax fibres *J. Compos. Mater.* **48** 1699–707
- [37] Placet V, Cisse O and Boubakar M L 2012 Influence of environmental relative humidity on the tensile and rotational behaviour of hemp fibres *J. Mater. Sci.* **47** 3435–46
- [38] Nuez L, Richely E, Perez J, Guessasma S, Beaugrand J, D'Arras P, Bourmaud A and Baley C 2022 Exploring the effect of relative humidity on dynamic evolution of flax fibre's microfibril angle through in situ tensile tests under synchrotron X-ray diffraction *Ind. Crops Prod.* **188** 115592
- [39] Drozdov A D 2010 Effect of temperature on the viscoelastic and viscoplastic behavior of polypropylene *Mech. Time-Dependent Mater.* **14** 411–34
- [40] Tripathi D 2002 *Practical Guide to Polypropylene* (Shropshire: RAPRA Technology)
- [41] Van de Velde K and Kiekens P 2001 Thermoplastic polymers: overview of several properties and their consequences in flax fibre reinforced composites *Polym. Test.* **20** 885–93
- [42] Zhou Y and Mallick P K 2002 Effects of temperature and strain rate on the tensile behavior of unfilled and talc-filled polypropylene. Part I: Experiments *Polym. Eng. Sci.* **42** 2449–60